
White Rose Research Online

eprints@whiterose.ac.uk
https://eprints.whiterose.ac.uk
Universities of Leeds, Sheffield and York

Deposited via The University of Sheffield.

White Rose Research Online URL for this paper:
https://eprints.whiterose.ac.uk/id/eprint/149786/

Version: Accepted Version

Proceedings Paper:
Masud, Z., Paspatis, A.G. and Konstantopoulos, G.C. (2019) Current-limiting droop controller for single-phase inverters operating in island mode. In: 45th Annual Conference of the IEEE Industrial Electronics Society (IECON 2019) Proceedings. 45th Annual Conference of the IEEE Industrial Electronics Society (IECON 2019), 14-17 Oct 2019, Lisbon, Portugal. IEEE, pp. 1659-1664. ISBN: 978-1-7281-4878-6. ISSN: 2577-1647.

https://doi.org/10.1109/IECON.2019.8926865

© 2019 IEEE. Personal use of this material is permitted. Permission from IEEE must be obtained for all other users, including reprinting/ republishing this material for advertising or promotional purposes, creating new collective works for resale or redistribution to servers or lists, or reuse of any copyrighted components of this work in other works. Reproduced in accordance with the publisher's self-archiving policy.

Reuse
Items deposited in White Rose Research Online are protected by copyright, with all rights reserved unless indicated otherwise. They may be downloaded and/or printed for private study, or other acts as permitted by national copyright laws. The publisher or other rights holders may allow further reproduction and re-use of the full text version. This is indicated by the licence information on the White Rose Research Online record for the item.

Takedown
If you consider content in White Rose Research Online to be in breach of UK law, please notify us by emailing eprints@whiterose.ac.uk including the URL of the record and the reason for the withdrawal request.



Current-Limiting Droop Controller for Single-Phase Inverters Operating in Island Mode

Zujajah Masud, Alexandros G. Paspatis and George C. Konstantopoulos
Dept. of Automatic Control & Systems Engineering
The University of Sheffield
Sheffield, UK
{zmasud1, apaspatis1, g.konstantopoulos}@sheffield.ac.uk

***Abstract*—In this paper, a current-limiting droop controller with nonlinear dynamics is proposed for the stand-alone operation of single-phase inverters. The proposed controller regulates the voltage and frequency of the load depending on the real and reactive power demand, as required in modern ac microgrids. The dynamic performance of inverters equipped with the proposed control scheme is investigated under different load conditions (linear and non-linear loads) and their current-limiting property is analytically proven to hold at all times using nonlinear ultimate boundedness theory. Then, the closed-loop stability of a single-phase inverter operating in island mode is proven for the first time using both a resistive and a constant power load. The desired controller performance is experimentally validated on a testbed consisting of a single-phase inverter connected to a linear (resistive) and a nonlinear (diode rectifier) load, where the ability of the proposed controller to operate in the droop control mode while maintaining the desired current limitation is proven under various load changes.**

***Index Terms*—Nonlinear control, single-phase inverter, current limitation, stability analysis**

I. Introduction

The decrease in fossil fuel reserves and associated environmental degradation has led to a significant increase of the renewable energy sources (RES) integration into the main grid in the last decades. This has subsequently increased the number of inverter interfaced units in the power network, since inverters represent the interface devices for RES. However, the inclusion of renewable based distributed generation (DG) units has affected the power flow and system stability, leading to a 70% reduction of the system strength of the UK grid within the next 20 years, as reported by National Grid's forecast [1]. Thus, advanced control techniques for the power inverter-interfaced DG units are required to ensure a reliable and stable operation of the power grid at all times.

Among the various methods proposed in literature to support the grid voltage and frequency [2]-[4], droop control is the most commonly used control strategy for inverter-interfaced DG units since ancillary services can be provided to the grid without the need of communication between the different DG units [5]-[6]. Several modifications in the droop control structure and dynamics have been proposed in the literature to improve the performance of the conventional droop controller by changing the droop coefficients or introducing different output impedances [7]-[9].

The stable operation of these control methods has been investigated based mainly on the small-signal model of the system and using root-locus analysis, which is valid for a given set of the system parameters. In stand-alone inverters or islanded microgrid applications, stability analysis has been conducted by considering linear load dynamics [10]-[11]. However, different types of loads, e.g. constant power loads (CPLs), have been shown to yield instability. Recently, several researchers have investigated the stability of inverters feeding a CPL depending on the ac microgrid architecture [12] or using Popov's criterion [13]. However, the stability of droop-controlled inverters connected to a CPL requires further investigation due to the inherent nonlinear structure and dynamics of the droop control scheme.

In addition, a crucial current-limiting property needs to be integrated along with the droop functions to ensure safe and reliable operation of every inverter unit. This will ensure that the inverter current will remain below a specified safe limit during normal and faulty grid conditions. To achieve this, external limiters or saturation units can be utilized to maintain the inverter current within safe range [14]-[16]. However, this can lead to oscillations and possible instability after the saturation limit is reached. Alternatively, low-voltage ride through structures can be utilized to ensure limited current injection during grid faults [17]. Moreover, additional protection devices [18] or adaptive relay algorithms [19] can be employed to protect the system from overcurrent conditions. These methods lack from rigorous stability proof and involve an external circuit in addition to the controller. To overcome this issue via the control design, a current-limiting droop controller has been proposed in [6] for grid-connected inverters, which maintains the inverter current below a maximum limit at all times. However, the same structure cannot be applied to an inverter operating in island mode under different load scenarios (e.g. CPL), which can result from a failure of main power grid due to an unexpected disturbance or fault [20]-[22].

In this paper, a new nonlinear current-limiting droop control method is proposed for a single-phase inverter operating in island mode. The inverter is considered to be connected to generic load (linear/nonlinear) via an LC filter. Initially, based on the nonlinear structure of the proposed controller and using ultimate boundedness theory, it is proven that the inverter current will never exceed a specified limit independently of the

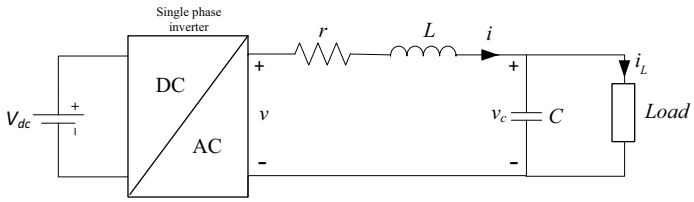

Fig. 1. A single-phase inverter in island mode.

load connected at its output. Then, the closed-loop stability of the system is investigated for two different cases: i) a resistive and ii) a constant power load. It is shown that any equilibrium point within the bounded operating range is asymptotically stable for an inverter equipped with the proposed current-limiting droop control; thus paving the way for proving stability in future microgrids. Several experimental results are presented to validate the performance of the proposed controller and its current-limiting property under varying load conditions for both a linear and a non-linear load. Compared to [6], where an inverter connected to a stiff grid is considered and system stability is not proven, in this paper, the desired operation and the asymptotic stability and current-limiting properties of a stand alone current-limiting droop controlled inverter, are shown for first time.

The rest of the paper is organized as follows: The dynamic model of a single-phase inverter operating in island mode and the proposed current-limiting droop controller are provided in Section II. The current-limiting property and the asymptotic stability of the closed-loop system are analytically proven for both a resistive and constant power load in Section III. Then, experimental results are presented and explained in Section IV to verify the desired performance of the proposed controller on a real inverter setup. Finally, some conclusions are drawn in Section V.

II. Controller Design

The system under consideration is an inverter unit in island mode, as shown in Fig. 1. It consists of a single-phase inverter connected to a generic load via an *LC* filter. The LC filter's inductance and capacitance are denoted by L and C respectively. Whereas, r represents the small parasitic resistance of the inductance. The inverter output voltage and current are v and i; while v_c is the capacitor voltage and i_L is the load current.

The dynamics of this system are given as:

$$L\frac{di}{dt} = -ri + v - v_c \tag{1}$$

$$C\frac{dv_c}{dt} = i - i_L, \tag{2}$$

where the controller input is considered as the inverter voltage v. Inspired by the current-limiting droop control structure presented in [6] for grid-connected inverters where a bounded variable virtual resistance is used, in this paper, the control scheme is extended to match the application of inverters in island mode as follows:

$$v = v_c + \sqrt{2}E^* \sin\theta - wi \tag{3}$$

where E^* is the rated RMS value of the load voltage, while θ is the inverter phase and w is a varying virtual resistance which are obtained from the following expressions:

$$\dot{w} = -c_w(K_e(E^* - V_c) - nP)w_q^2 \tag{4}$$

$$\begin{aligned}\dot{w_q} = &\frac{c_w(w - w_m)w_q}{\triangle w_m^2}(K_e(E^* - V_c) - nP) \\ &- k_w\left(\frac{(w - w_m)^2}{\triangle w_m^2} + w_q^2 - 1\right)w_q\end{aligned} \tag{5}$$

$$\dot{\theta} = \omega^* + mQ, \tag{6}$$

where w_q is an additional controller state, c_w, w_m, Δw_m, k_w and K_e are positive constant quantities, V_c is the RMS capacitor (load) voltage, P and Q represent the average active and reactive power delivered by the inverter. In addition, n are m are the droop coefficients and ω^* corresponds to the rated value of angular frequency. Since $\dot{\theta} = \omega$, where ω is the frequency of the inverter, it is desired at the steady state to have

$$V_c = E^* - \frac{nP}{K_e} \tag{7}$$

$$\omega = \omega^* + mQ, \tag{8}$$

which represent the droop expressions of an inverter with resistive output impedance in island mode. As it has been shown in [6], by selecting the initial conditions $w_0 = w_m$ and $w_{q0} = 1$ for the controller states, the varying virtual resistance w is always positive and bounded in the range $w \in [w_{min}, w_{max}] > 0$, where $w_{min} = w_m - \Delta w_m > 0$ and $w_{max} = w_m + \Delta w_m > 0$. For more details, the reader is referred to [6]. This concept of boundedness has also been investigated in [23]-[24].

III. Stability Analysis

A. Current-Limiting Property

In order to analyze the current-limiting property of the inverter in island mode, the controller proposed in (3) is substituted into the plant dynamics given by (1). Then, the closed-loop current dynamics become

$$L\frac{di}{dt} = -(r + w)i + \sqrt{2}E^* \sin\theta. \tag{9}$$

For the analysis, the energy stored in the inductor can be considered as a candidate Lyapunov function

$$V = \frac{1}{2}Li^2. \tag{10}$$

By taking the time derivative of V and cosidering that $w \in [w_{min}, w_{max}] > 0$ holds true from the proposed controller dynamics, it yields that

$$\begin{aligned}\dot{V} &= -(r + w)i^2 + \sqrt{2}E^* i \sin\theta \\ &\leq -(r + w_{min}) \mid i \mid^2 + \sqrt{2}E^* \mid i \mid\mid \sin\theta \mid .\end{aligned}$$

The above inequality reveals that $\dot{V} \leq -r \mid i \mid^2$ if

$$w_{min} \mid i \mid^2 \geq \sqrt{2}E^* \mid i \mid$$

or

$$\mid i \mid \geq \frac{\sqrt{2}E^*}{w_{min}}. \tag{11}$$

Since $r \mid i \mid^2$ is a continuous positive definite function, then from Theorem 4.18 [25], there exists a class KL function β and for every initial state $i(0)$, there is $T \geq 0$ such that the solution of inverter current $i(t)$ satisfies

$$\mid i(t) \mid \leq \beta(i(0), t), \qquad \forall\, 0 \leq t \leq T$$
$$\mid i(t) \mid \leq \frac{\sqrt{2}E^*}{w_{min}}, \qquad \forall\, t \geq T$$

As a result, the solution of the inverter current $i(t)$ is uniformly ultimately bounded and therefore if at $t = 0$ it holds true that

$$\mid i(0) \mid \leq \frac{\sqrt{2}E^*}{w_{min}},$$

then $T = 0$ and the solution $i(t)$ will remain below the same value for all future time, i.e.

$$\mid i(t) \mid \leq \frac{\sqrt{2}E^*}{w_{min}}, \quad \forall\, t \geq 0. \tag{12}$$

Now, if w_{min}, which is a controller parameter, is chosen as

$$w_{min} = \frac{E^*}{I_{max}} \tag{13}$$

where I_{max} is the maximum RMS value of the inverter current (positive constant), then by substituting (13) in (12), it yields

$$\mid i(t) \mid \leq \frac{\sqrt{2}E^*}{\frac{E^*}{I_{max}}}, \quad \forall\, t \geq 0 \tag{14}$$

or

$$\mid i(t) \mid \leq \sqrt{2}I_{max}, \quad \forall\, t \geq 0. \tag{15}$$

Considering that $i(t) = \sqrt{2}I \sin\phi$, where I and ϕ are the RMS value and phase angle of the inverter current, respectively, then since (15) holds true for all $t \geq 0$, there is

$$I(t) < I_{max}, \quad \forall\, t \geq 0. \tag{16}$$

The above inequality shows that the desired current-limiting property is maintained by the proposed controller for any inverter operating in island mode without depending on the load characteristics or the filter parameters. Hence, the current-limitation is guaranteed for any load, i.e. linear or nonlinear, and even under faulty load conditions (short circuits or faults), which is a unique characteristic of the proposed design.

B. Asymptotic Stability

Although the current-limiting property of the inverter is guaranteed by the previous analysis, the asymptotic convergence to the desired equilibrium is yet to be proven. To proceed with the stability analysis, two different load cases are considered: i) a resistive and ii) a constant power load.

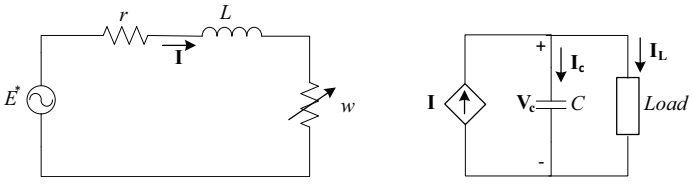

Fig. 2. Alternative circuit for single-phase inverter connected to a generic load in island mode.

1) Resistive Load: When a resistive load is considered at the output of the inverter, the closed-loop system dynamics are obtained by considering that $i_L = \frac{v_c}{R}$ and applying (3) into (1)-(2) as:

$$L\frac{di}{dt} = -ri + \sqrt{2}E^* \sin\theta - wi \tag{17}$$
$$C\frac{dv_c}{dt} = i - \frac{v_c}{R} \tag{18}$$

in addition to the controller dynamics (4)-(6). Since the average values of the real power P and the reactive power Q are required in the controller dynamics, these can be obtained using the phasor quantities of the capacitor voltage $\mathbf{V_c}$ and the inverter current $\mathbf{I}$. It should be noted that different time scales are considered for the voltage and frequency dynamics as in [26], and thus frequency can be considered as constant to investigate system stability through phasors modeling. Since the inverter frequency $\omega = \dot{\theta}$ is given from the static expression (6), then the closed-loop system dynamics can be alternatively represented by a coupled circuit as shown in Fig. 2, where w is varying according to (4)-(5). Hence, for the stability analysis, the dynamics of w and w_q are needed to be investigated where V_c and P are written as functions of w and w_q. To proceed with the analysis, the input voltage of the closed-loop system shown in Fig. 2 is considered as reference, i.e. $E^* \angle 0$. Then the phasor inverter current $\mathbf{I}$ can be calculated as:

$$\mathbf{I} = \frac{E^*}{\sqrt{(r+w)^2 + (X_L)^2}} \angle -\tan^{-1}\left(\frac{X_L}{r+w}\right) \tag{19}$$

while the phasor capacitor voltage $\mathbf{V}_c$ results in:

$$\mathbf{V_c} = \frac{E^*}{\sqrt{(r+w)^2 + (X_L)^2}\sqrt{(\frac{1}{R})^2 + (\frac{1}{X_c})^2}} \angle -\tan^{-1}\left(\frac{X_L}{r+w}\right) - \tan^{-1}\left(\frac{R}{X_c}\right). \tag{20}$$

The real power P is calculated as $P = Re\{\mathbf{V_c}\mathbf{I}^*\}$ and results after some calculations is the following expression:

$$P = \frac{E^{*2}}{\Big((r+w)^2 + (X_L)^2\Big)\sqrt{(\frac{1}{R})^2 + (\frac{1}{X_c})^2}} \cos\Big(\tan^{-1}\left(\frac{R}{X_c}\right)\Big) \tag{21}$$

where X_L and X_C are the reactances of the LC filter's inductance and capacitance respectively. By substituting the RMS value V_c of capacitive voltage, which is the magnitude of the phasor $\mathbf{V}_c$ given by (20), and real power P from (21) into the controller dynamics (4) and (5), it results in:

$$\begin{aligned}\dot{w} = & -c_w\Bigg[K_e\Bigg(E^* - \frac{E^*}{\sqrt{(r+w)^2+(X_L)^2}\sqrt{(\frac{1}{R})^2+(\frac{1}{X_c})^2}}\Bigg) \\ & - \frac{nE^{*2}}{\big[(r+w)^2+(X_L)^2\big]\sqrt{(\frac{1}{R})^2+(\frac{1}{X_c})^2}}\cos\big(\tan^{-1}(\frac{R}{X_c})\big)\Bigg]w_q^2\end{aligned} \tag{22}$$

$$\begin{aligned}\dot{w_q} = & \frac{c_w(w-w_m)w_q}{\triangle w_m^2}\Bigg[K_e\Bigg(E^* - \frac{E^*}{\sqrt{(r+w)^2+(X_L)^2}\sqrt{(\frac{1}{R})^2+(\frac{1}{X_c})^2}}\Bigg) \\ & - \frac{nE^{*2}}{\big[(r+w)^2+(X_L)^2\big]\sqrt{(\frac{1}{R})^2+(\frac{1}{X_c})^2}}\cos\big(\tan^{-1}(\frac{R}{X_c})\big)\Bigg] \\ & - k_w\Bigg(\frac{(w-w_m)^2}{\triangle w_m^2} + w_q^2 - 1\Bigg)w_q\end{aligned} \tag{23}$$

which shows that the controller states form a non-linear system of form

$$\dot{x} = f(x) \tag{24}$$

where $x = \begin{bmatrix} w & w_q \end{bmatrix}^\top$ is a state vector.

Since it has been proven that the solution of the nonlinear system (24) is bounded with $w \in [w_{min}, w_{max}]$ and $w_q \in [0, 1]$ (for details see [6]), then consider any equilibrium point (w_e, w_{q_e}) where $w_e \in (w_{min}, w_{max}) > 0$ and $w_{q_e} \in (0, 1]$ for which the droop expressions (7) and (8) are satisfied. Then the Jacobian matrix of the closed-loop system defined by (22)-(23) has the following two eigenvalues:

$$\begin{aligned}\lambda_1 = & -c_w\Bigg(\frac{K_e(r+w_e)}{(r+w_e)^2+(X_L)^2}V_{ce} \\ & + \frac{2n(r+w_e)}{(r+w_e)^2+(X_L)^2}P_e\Bigg)w_{qe}^2\end{aligned} \tag{25}$$

$$\lambda_2 = -2k_w w_{qe}^2, \tag{26}$$

where V_{ce} and P_e are the values of RMS capacitor voltage and the real power at the equilibrium $w = w_e$. Since $w_e > 0$ and all parameters K_e, X_c, X_L, r, n, R and E^* are positive constants, then the RMS value of capacitive voltage V_c and real power P are guaranteed to be positive. Therefore, $\lambda_1 < 0$ as c_w is a positive constant. Moreover, $\lambda_2 < 0$ since k_w is a positive constant and $w_{qe} \in (0, 1]$. Hence all the eigenvalues of the Jacobian matrix have strictly negative real parts and every equilibrium point (w_e, w_{q_e}) of the closed-loop system defined in the bounded range is proven to be asymptotically stable.

2) Constant Power Load: In this case, the load connected to a single-phase inverter is considered to be a constant power load, i.e. the load draws a constant power $P_L > 0$ at all times, which means that the plant dynamics are now given as:

$$L\frac{di}{dt} = -ri + v - v_c \tag{27}$$

$$C\frac{dv_c}{dt} = i - \frac{P_L}{v_c} \tag{28}$$

The closed-loop stability of this system is established in a similar manner as in the case of resistive load. The eigenvalues of the Jacobian matrix, for the case of constant power load, at the equilibrium point are given as:

TABLE I
SYSTEM AND CONTROLLER PARAMETERS

Parameters	Values	Parameters	Values
L	7 mH	I_{max}	2 A
C	11 μF	I_{min}	0.1 A
E^*	40 V	K_e	10
ω^*	2π x 50 rad/s	k_w	1000

$$\begin{aligned}\lambda_1 = & -c_w w_{qe}^2\Bigg[\frac{1}{2}X_c^2K_e\frac{1}{V_{ce}}\Bigg[\Bigg(\frac{E^{*2}(r+w_e)}{\big((r+w_e)^2+(X_L)^2\big)^2}\Bigg) \\ & + \frac{\frac{E^{*4}(r+w_e)}{\big((r+w_e)^2+X_L^2\big)^3}}{\sqrt{\Bigg(\big(\frac{E^{*2}}{(r+w_e)^2+(X_L)^2}\big)^2 - 4\frac{P_L^2}{X_c^2}\Bigg)}}\Bigg]\Bigg]\end{aligned} \tag{29}$$

$$\lambda_2 = -2k_w w_{qe}^2. \tag{30}$$

Similar to the analysis of the case with a resistive load, both eigenvalues of the Jacobian matrix have negative real parts, proving the asymptotic stability of any equilibrium point in the bounded range. However, in order for the equilibrium point (w_e, w_{q_e}) to exist in the range where $w_e \in (w_{min}, w_{max}) > 0$, the expression inside the square root in (29) should be positive, i.e.

$$\Bigg(\frac{E^{*2}}{(r+w_e)^2+X_L^2}\Bigg)^2 - 4\frac{P_L^2}{X_c^2} > 0.$$

Since the above inequality should hold for all $w_e \in (w_{min}, w_{max}) > 0$, then:

$$w_{max} < \sqrt{\frac{E^{*2}X_c}{2P_L} - X_L^2} - r. \tag{31}$$

Inequality (31) provides guidance on the selection of the controller parameter w_{max}. Combined with the selection of w_{min} from (13), the control parameters w_m and Δw_m are defined from $w_m = (w_{max}+w_{min})/2$ and $\Delta w_m = (w_{max}-w_{min})/2$. When P_L is unknown, w_{max} can be selected according to the minimum current I_{min} flowing through the LC filter as $w_{max} = E^*/I_{min}$.

IV. EXPERIMENTAL RESULTS

In order to validate the performance of the proposed current-limiting droop controller, experiments were carried out on a S_n=220 VA single-phase inverter operating in island mode for different load conditions. The single-phase inverter is powered by a 100 V DC and operated at a switching frequency of 15kHz. The controller was implemented on the TI F28M35H52C1 microcontroller with a sampling frequency of 4 kHz. The system and controller parameters are shown in Table I. The desired voltage drop ratio and frequency boost ratio are chosen as 5% and 1% respectively. This results in the droop coefficients as $n = 0.05K_eE^*/S_n$ and $m = 0.01\omega^*/S_n$. Moreover, w_m is calculated as $\frac{w_{min}+w_{max}}{2}$; where w_{min} and w_{max} are evaluated as $\frac{E^*}{I_{max}}$ and $\frac{E^*}{I_{min}}$, respectively. The inverter is tested for both a linear (resistive) load and a non-linear (diode rectifier) load.

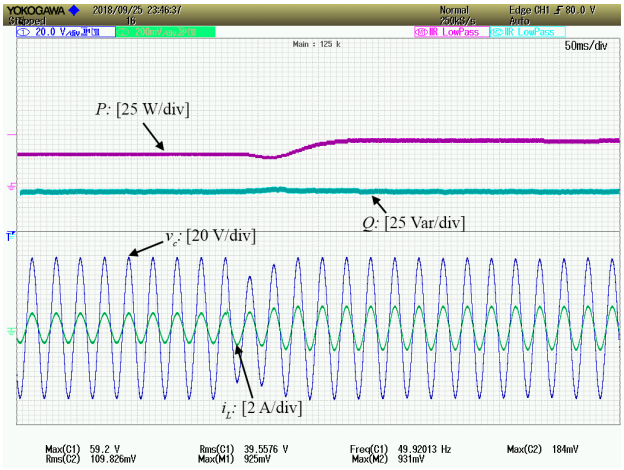

Fig. 3. Transient response under linear load change from 50 Ω to 33 Ω.

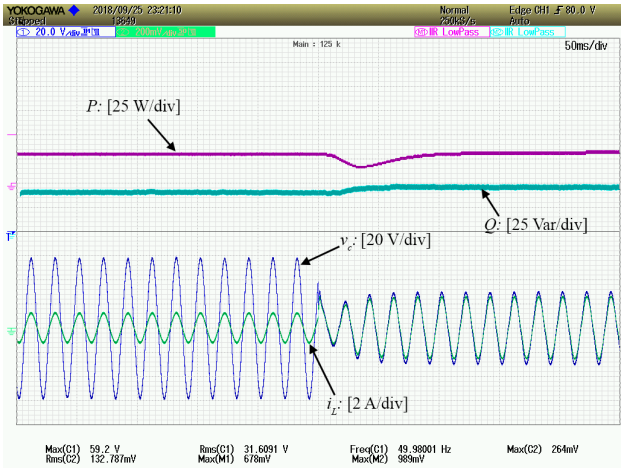

Fig. 4. Transient response under linear load change from 50 Ω to 12 Ω.

A. Linear Load

In this case, the single-phase inverter is connected to a resistive load. Initially, it is operated at a load of 50 Ω and then the load changes to 33 Ω. The transient response of the inverter during load change is shown in Fig. 3. The controller successfully regulates the load voltage close to rated voltage of 40 V due to the droop expression after the sudden load change, as can be seen in Fig. 3. During the transient, the inverter current increases gradually in response to the load increase. Thus, load voltage drops at first and then rises back to its desired value. Since load and inverter current has increased, the active power also rises following the load change. Whereas, the reactive power returns close to its initial value after a short transient as load voltage returns to close its nominal value. This is clearly depicted at the upper half of Fig. 3.

In order to test the controller performance and its current-limiting property under higher load power demand, the inverter is tested under a sudden load change from 50 Ω to 12 Ω. The transient response of the inverter during this load change is shown in Fig. 4. As can be seen, the load voltage is regulated to its rated value prior to load change. However, the load voltage is seen to drop from its rated value for a load of 12 Ω. This is due to the fact that such an increase in load demands an inverter current higher than I_{max} to achieve the droop control regulation. Hence, the controller limits the inverter current to a value lower than I_{max}, as theoretically proven in the paper. As seen in Fig. 4, the RMS value of inverter current is limited to around 1.7 A. This value is slightly lower than the specified maximum of 2 A due to the non-zero parasitic resistance of the filter inductance; however the current still remains below the desired value. Moreover, the real and reactive power also decrease following the load change since the load voltage drops due to the loading effect, seen clearly in Fig. 4.

B. Non-linear Load

In the second scenario, the performance of the proposed controller is validated for a non-linear load by connecting the single-phase inverter to a resistive load via a diode bridge rectifier. This setup is initially operated at a load of 100 Ω and then the load is switched to 32 Ω. The response of the inverter during this transition is shown in Fig. 5. As seen in the figure, the controller regulates the load voltage slightly below the rated value of 40 V defined by the term $\frac{nP}{K_e}$ as expected by the droop controller both before and after the load change. The active power increases due to the decrease in the load resistance as seen in Fig. 5. The reactive power also slightly changes due to the fact that the inverter current is not purely sinusoidal for the non-linear load case. Note that the reactive power is calculated using the inverter and not the load current.

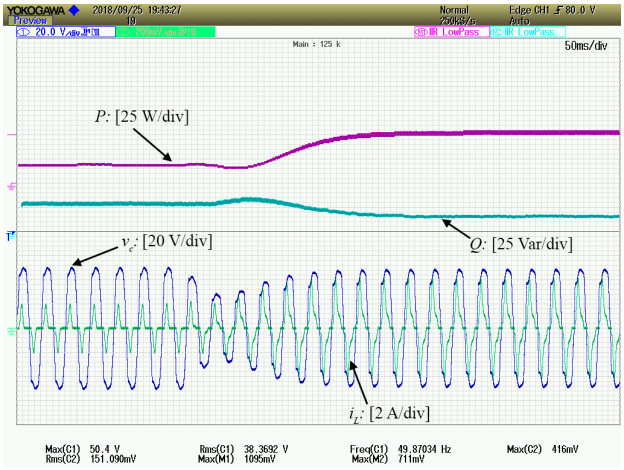

Fig. 5. Transient response under non-linear load change from 100 Ω to 32 Ω.

Later, the load is suddenly changed to a value of 25 Ω from 100 Ω and the response during this transition is shown in Fig. 6. Similar to the case of the linear load, the load voltage is regulated to its desired value before the change of load. However, after the change of the load resistance, the load voltage is seen to be lower than its rated value. This is due to inverter current being limited to lower than I_{max} and hence protecting the inverter from high currents that can damage the device, by automatically sacrificing the

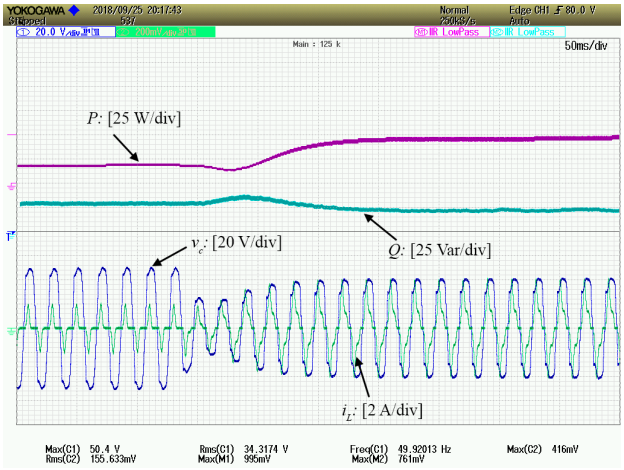

Fig. 6. Transient response under non-linear load change from 100 Ω to 25 Ω.

droop control regulation. This demonstrates the ability of the proposed controller to limit the inverter current within specified range for any type of linear or non-linear load.

V. Conclusion

In this paper, a droop controller with current-limiting property has been proposed for the stand-alone single-phase inverter operation. The proposed controller was able to achieve the desired real and reactive power droop functions with tight load voltage regulation. Moreover, the closed-loop stability of the system under consideration was proven for both linear and non-linear loads, including the constant power load case. Additionally, it has been demonstrated that controller maintains the inverter current within a specified range at all times. The performance of the controller and its current-limiting property were verified by a set of experimental results.

Acknowledgment

This work is supported by EPSRC under Grant No.EP/S001107/1.

References

[1] National Grid, Electricity Ten Year Statement 2014.

[2] F. Blaabjerg, R. Teodorescu, M. Liserre, and A. V. Timbus, "Overview of control and grid synchronization for distributed power generation systems," *IEEE Transactions on industrial electronics*, vol. 53, no. 5, pp. 1398–1409, 2006.

[3] Q. Zeng and L. Chang, "Study of advanced current control strategies for three-phase grid-connected pwm inverters for distributed generation," in *Proceedings of 2005 IEEE Conference on Control Applications, 2005. CCA 2005.*, pp. 1311–1316, Aug 2005.

[4] P. C. Loh and D. G. Holmes, "Analysis of multiloop control strategies for lc/cl/lcl-filtered voltage-source and current-source inverters," *IEEE Transactions on Industry Applications*, vol. 41, pp. 644–654, March 2005.

[5] Q.-C. Zhong and T. Hornik, *Control of power inverters in renewable energy and smart grid integration*, vol. 97. John Wiley & Sons, 2012.

[6] Q.-C. Zhong and G. C. Konstantopoulos, "Current-limiting droop control of grid-connected inverters," *IEEE Transactions on Industrial Electronics*, vol. 64, no. 7, pp. 5963–5973, 2017.

[7] J. C. Vasquez, J. M. Guerrero, A. Luna, P. Rodriguez, and R. Teodorescu, "Adaptive droop control applied to voltage-source inverters operating in grid-connected and islanded modes," *IEEE Transactions on Industrial Electronics*, vol. 56, pp. 4088–4096, Oct 2009.

[8] E. de Paiva, J. Vieira Jr, L. de Freitas, V. Farias, and E. Coelho, "An improved power controller for a single phase grid connected inverter with root locus analysis," *Revista Eletrônica de Potência–SOBRAEP, Campinas*, vol. 14, no. 1, pp. 17–23, 2009.

[9] W. Yao, M. Chen, J. Matas, J. M. Guerrero, and Z. Qian, "Design and analysis of the droop control method for parallel inverters considering the impact of the complex impedance on the power sharing," *IEEE Transactions on Industrial Electronics*, vol. 58, pp. 576–588, Feb 2011.

[10] A. U. Krismanto and N. Mithulananthan, "Identification of modal interaction and small signal stability in autonomous microgrid operation," *IET Generation, Transmission Distribution*, vol. 12, no. 1, pp. 247–257, 2018.

[11] N. Pogaku, M. Prodanovic, and T. C. Green, "Modeling, analysis and testing of autonomous operation of an inverter-based microgrid," *IEEE Transactions on Power Electronics*, vol. 22, pp. 613–625, March 2007.

[12] D. Semënov, G. Mirzaeva, C. D. Townsend, and G. C. Goodwin, "An ac microgrid architecture and control strategy to achieve stability with any type of load," in *2017 IEEE Southern Power Electronics Conference (SPEC)*, pp. 1–6, Dec 2017.

[13] D. Karimipour and F. R. Salmasi, "Stability analysis of ac microgrids with constant power loads based on popov's absolute stability criterion," *IEEE Transactions on Circuits and Systems II: Express Briefs*, vol. 62, no. 7, pp. 696–700, 2015.

[14] C. A. Plet, M. Brucoli, J. D. McDonald, and T. C. Green, "Fault models of inverter-interfaced distributed generators: Experimental verification and application to fault analysis," 2011.

[15] T. Dragicevic, J. M. Guerrero, J. C. Vasquez, and D. Skrlec, "Supervisory control of an adaptive-droop regulated dc microgrid with battery management capability," *IEEE Trans. Power Electron*, vol. 29, no. 2, pp. 695–706, 2014.

[16] A. D. Paquette and D. M. Divan, "Virtual impedance current limiting for inverters in microgrids with synchronous generators," *IEEE Transactions on Industry Applications*, vol. 51, no. 2, pp. 1630–1638, 2015.

[17] Y. Yang, F. Blaabjerg, and H. Wang, "Low-voltage ride-through of single-phase transformerless photovoltaic inverters," *IEEE Transactions on Industry Applications*, vol. 50, pp. 1942–1952, May 2014.

[18] H. J. Laaksonen, "Protection principles for future microgrids," *IEEE Transactions on Power Electronics*, vol. 25, pp. 2910–2918, Dec 2010.

[19] M. A. Haj-ahmed and M. S. Illindala, "The influence of inverter-based dgs and their controllers on distribution network protection," *IEEE Transactions on Industry Applications*, vol. 50, pp. 2928–2937, July 2014.

[20] Y. Chen, R. Hesse, D. Turschner, and H.-P. Beck, "Investigation of the virtual synchronous machine in the island mode," in *Innovative Smart Grid Technologies (ISGT Europe), 2012 3rd IEEE PES International Conference and Exhibition on*, pp. 1–6, IEEE, 2012.

[21] G. C. Konstantopoulos, Q. Zhong, B. Ren, and M. Krstic, "Bounded integral control of input-to-state practically stable nonlinear systems to guarantee closed-loop stability.," *IEEE Trans. Automat. Contr.*, vol. 61, no. 12, pp. 4196–4202, 2016.

[22] M. A. Pedrasa and T. Spooner, "A survey of techniques used to control microgrid generation and storage during island operation," *AUPEC2006*, vol. 1, p. 15, 2006.

[23] A. G. Paspatis, G. C. Konstantopoulos, M. Mayfield, and V. C. Nikolaidis, "Current-limiting droop controller with fault-ride-through capability for grid-tied inverters," in *2017 IEEE PES Innovative Smart Grid Technologies Conference Europe (ISGT-Europe)*, pp. 1–6, Sept 2017.

[24] G. C. Konstantopoulos, Q. Zhong, B. Ren, and M. Krstic, "Bounded integral control of input-to-state practically stable nonlinear systems to guarantee closed-loop stability," *IEEE Transactions on Automatic Control*, vol. 61, pp. 4196–4202, Dec 2016.

[25] H. K. Khalil and J. W. Grizzle, *Nonlinear systems*, vol. 3. Prentice hall Upper Saddle River, NJ, 2002.

[26] Q. Zhong, G. C. Konstantopoulos, B. Ren, and M. Krstic, "Improved synchronverters with bounded frequency and voltage for smart grid integration," *IEEE Transactions on Smart Grid*, vol. 9, pp. 786–796, March 2018.